Geo.Alp, Vol. 9, S. 82–99, 2012

TALUS ACCUMULATION IN DETACHMENT SCARS OF LATE HOLOCENE ROCK AVALANCHES, EASTERN ALPS (AUSTRIA): RATES AND IMPLICATIONS.

Diethard Sanders

With 6 Figures and 3 Tables

Institute for Geology and Paleontology, University of Innsbruck, Innrain 52, A-6020 Innsbruck, Austria
Email: Diethard.G.Sanders@uibk.ac.at

To Lorenz
Heaven and Earth are indifferent; They take the tenthousand Beings as Dummies
(Lao-Dse 5, 13)

Abstract

In mountain ranges, under the present interglacial conditions, active scree slopes tend to cluster within a certain range of altitude, probably because of an altitudinal/climatic span with maximum efficiency of frost cracking (‚talus window'). In the Northern Calcareous Alps, large active scree slopes within the detachment scars of two late Holocene rock avalanches accumulated at mean rates of 7–18 mm/a over a time interval of ~1.7–3.8 ka. A plot of sedimentation rates as a function of time interval (Sadler plot) shows: (a) that the two scree slopes accumulated at comparatively high rates, and that (b) the rate of deposition must have been much higher (up to ≥1 meter/a) shortly after rock avalanching, but then diminished. The apex of each scree slope is located close to 1400 m a.s.l., i. e. some 400–1000 meters lower in altitude than the apices of most other scree slopes of the Eastern Alps. At the time of rock avalanching, the mountain flank laterally adjacent to the scree slopes was forested up to its crest, as it is today. Climatic data (1971-2000) of stations ranging from 498–3105 m a.s.l. in altitude suggest that the intense scree production is not readily explained by the annual number of ice days (ID; days with T < 0°C). The annual number of freeze-thaw days (FTD), in contrast, remains nearly constant from station Haiming (695 m a.s.l.; 130 FTD) up to Obervermunt (2040 m a.s.l.; 125 FTD). Thus, scree production may have been mainly controlled by FTD or by, both, FTD and ID compensating in effect each other with increasing altitude. In addition, processes unrelated to freezing probably significantly contributed to scree production, such as ‚scraping' off scree by heavy rainfalls and snow cascading or avalanching down cliffs, spalling of rock by increased pore-water pressure, and rock cracking/loosening by thermal stress fatigue well-above the freezing point.

I suggest that the prevalence of presently-active scree slopes in a certain altitude range (slope apex between ~1800 to ~2600 m a.s.l.) of the Eastern Alps results from: (a) the gross topography across the orogen, with internides (Central Alps) the highest, (b) medium-scale morphology produced mainly by glacial erosion (cirques and glacially-carved valleys flanked by cliffs), (c) post-glacial climb of vegetation, superposed with (d) an optimal combination of all processes (irrespective of their total altitude range) capable to (i) liberate scree from cliffs, and (ii) at a combined rate high enough to sustain a sizeable, active scree slope. This interpretation does not invalidate, but embeds the concept of the ‚frost-cracking window'. In the Northern Calcareous Alps, observations on the long-term (here: > 10 ka) and short-term (here: tens of years) dynamics of talus accumulations indicate that the role of vegetation for scree shedding from cliffs (technically, rock flanks with dip ≥45°) has been underestimated. In the Alps, the scarcity of presently active talus below about 1600–2000 m a.s.l. mainly results from slope stabilization by vegetation rather than by lack of processes capable to liberate scree from bare rocky slopes. The two scree slopes described herein indicate that, under certain geological circumstances, rapid talus accumulation in comparatively low topographic position is possible also under interglacial climatic conditions.

Keywords: Alps, Holocene, talus, scree, accumulation rate, rock avalanche

Introduction

In the Northern Calcareous Alps (NCA), post last-Glacial talus situated in altitudes less than about 1600–1800 m a.s.l. most commonly is abandoned, covered by vegetation, and/or undergoes erosion while active scree slopes are located mainly between 1800–2600 m a.s.l. (Sanders and Ostermann, 2011). The gross vertical distribution of active scree slopes in mountain ranges is believed to reflect the position of an altitudinal-climatic range with maximum efficiency of frost cracking (‚talus window'; Hales and Roering, 2005). A brief look into satellite images of the Alps of course seems to support the concept of a talus window, as it is obvious that most active scree slopes are located within a specific range, more-or-less wide, of altitudes. On carbonate-lithic scree slopes of the Eastern Alps, aerial photographs (since 1946) and satellite imagery show that the modern climatic warming and humidification is reflected by: (a) upward climb of vegetation, (b) incision or lengthening of channels passed by ephemeral surface runoff, and (c) increased activity or nucleation of parasitic alluvial fans farther downslope (Konrad, 2010). As the altitude range of vegetation belts is controlled by climate, this observation goes along with the idea of a strong climatic influence on scree production. On the other hand, in the Alps, many active scree slopes are located in much lower altitudes. These low-positioned slopes are clearly controlled by structural features (faults, more-or-less wide zones of rock cataclasis, and slow gravitational slope deformations).

There exists perhaps no other depositional system with such a rigid negative feedback between sediment source area (=rock cliff) and accumulation area (=scree slope) as cliff/talus systems. In an ideal situation, talus accumulation starts with a plane, vertical cliff (t_0 in Fig. 1A) of relatively competent rocks degrading by parallel retreat (see Obanawa and Matsukura, 2006; Utili and Crosta, 2011, for discussion and references). In an early stage, the slope surface is of low dip, but steepens with time (e. g., Clowes and Comfort, 1987; Summerfield, 1991; Sanders et al., 2009). Upon steepening, a critical threshold of slope dip set by the angle of residual shear is attained that is not exceeded. For carbonate-lithic talus, this dip angle is typically ~35°. Because the cliff becomes gradually onlapped and buried, this results in an increasing disparity between sediment supply and accumulation area by autocyclic feedback. Because the surface between cliff and talus develops a convex shape (Fig. 1A) (e.g., Hutchinson, 1998; Utili and Crosta, 2011, among others), the free cliff area initially shrinks exponentially; later, when the talus dips with the angle of residual shear, the decrease of cliff surface per time increment is practically linear (red graph in Fig. 1B). Conversely, the length of the scree slope at first grows slowly but strives towards a practically linear increase later (black graph in Fig. 1B). Provided that no basal removal of scree and no cliff rejuvenation takes place, thus, talus deposition inexorably strives to fade out, independent of climate (Sanders, 2010). In addition, in the Alps, settings of post-last Glacial talus accumulation changed markedly: During rapid deglacial ice decay, very high glacially-weakened mountain flanks supplied copious scree to low-positioned alluvial fans and talus; upon climatic amelioration, with rise of the talus window and climb of vegetation, talus accumulation became confined to higher-located cirques and to a few high, more-or-less stabilized cliffs (Sanders and Ostermann, 2011). Post-glacial slowing of talus accumulation thus went hand-in-hand with the effects of deglacial to modern climatic changes.

So how to better discriminate potential controls over scree-slope development? In the Alps, deposits of rock avalanches are common; such events include extremely fast, gravity-driven mass-wasting of rock with an initial volume of $>10^5$ m^3 (Evans et al., 2006) or $>10^6$ m^3 (Erismann and Abele, 2001). Age-dating of rock avalanche events is mostly done by the radiocarbon method and/or by surface exposure dating (e. g., Patzelt and Poscher, 1993; Ivy-Ochs et al., 1998; Prager et al., 2008). The age of a rock avalanche event also dates the start of geomorphic changes triggered by mass-wasting, such as the accumulation of scree slopes within the detachment scar. Scree slopes in detachment scars of rock avalanches are widespread, yet they are only rarely exposed down to their base, to allow for an estimate of sediment accumulation rate. In the present paper, the time-scaled accumulation rates of talus formed in detachment scars of age-dated, late Holocene rock avalanches are compared with literature data on scree accumulation and cliff retreat. High time-scaled accumulation rates of the rock avalanche-related talus imply very fast deposition of scree closely after rock avalanche events. Talus accumulation in scars of historical rock avalanches also indicates that scree deposition associated with sudden defacement of cliffs is extremely non-linear in time. The accumulation rates of the rock avalanche-related scree slopes,

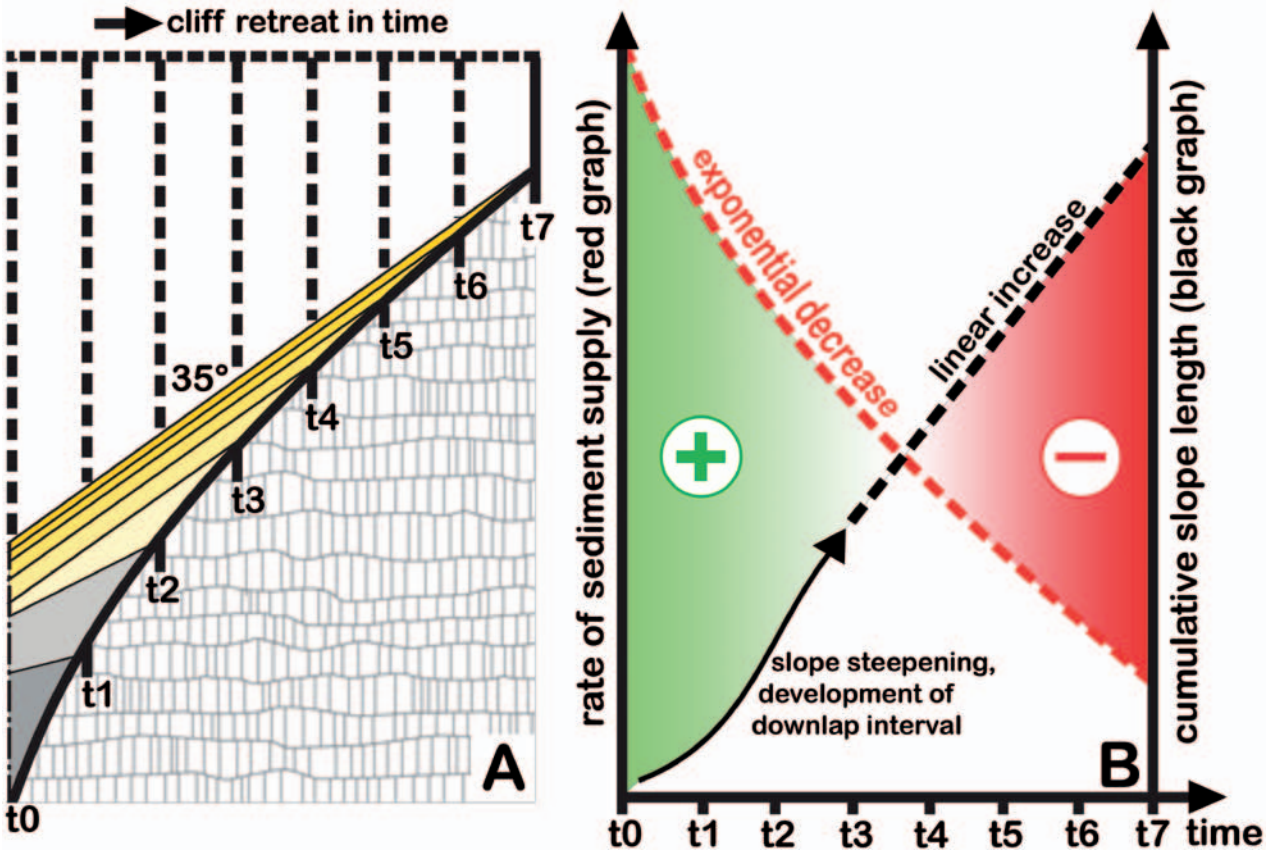

Fig. 1: Parallel cliff retreat and onlap of talus in time, starting at time t0. A. During cliff retreat, the talus surface steepens until the angle of residual shear of scree is attained (taken as 35°), here at time t3; this dip angle is not surpassed with further cliff retreat. Between the onlapping talus and the retreating cliff, a convex truncation surface forms. With time, the dip of the truncation surface strives towards the angle of residual shear of the scree slope. B. The development described in subfigure A results in: (1) an exponential decrease of cliff area and, hence, in sediment supply, while (2) slope length increases. The negative feedback between sediment supply and talus length defines an early stage with strongly positive sediment budget relative to slope length (green area labeled ‚plus'), and (b) a late stage with progressively less sediment available to supply an ever-larger slope area (red area labeled ‚minus'). See text for further outline and references.

however, compare well with rates from settings not influenced by rocksliding. Consideration of the altitude of the upper treeline ecoline at the times when the rock avalanches had detached, and a comparison of meteorological data (1971-2000) over a large altitude range suggest that intense scree production from the scars is not straightforwardly explained by the annual number of ice days (days with T < 0°C), but by annual number of freeze-thaw days and/or by erosional processes unrelated to frost. Moreover, the influence of vegetation cover on scree shedding from steep, rocky mountain flanks most probably has been underestimated. Considerations on long-term development of scree slopes and alluvial fans should take vegetation into account.

Methods

Each of the rock avalanches and subsequent talus slopes mentioned herein were inspected in the field. The thickness of post-rock avalanche talus successions exposed from bottom to top was determined by: (a) field measurement, and/or (b) by geometrical construction in isohypsed satellite orthoimages on a scale of 1/1000 (provided by the federal government of the Tyrol; www.tirol.gv.at/tiris). To determine a mean rate of talus accumulation since rocksliding, the thickness of talus successions in the detachment scars was divided by the mean ages of rock avalanche events (see below). To compare the calculated rates of talus accumulation with previously published va-

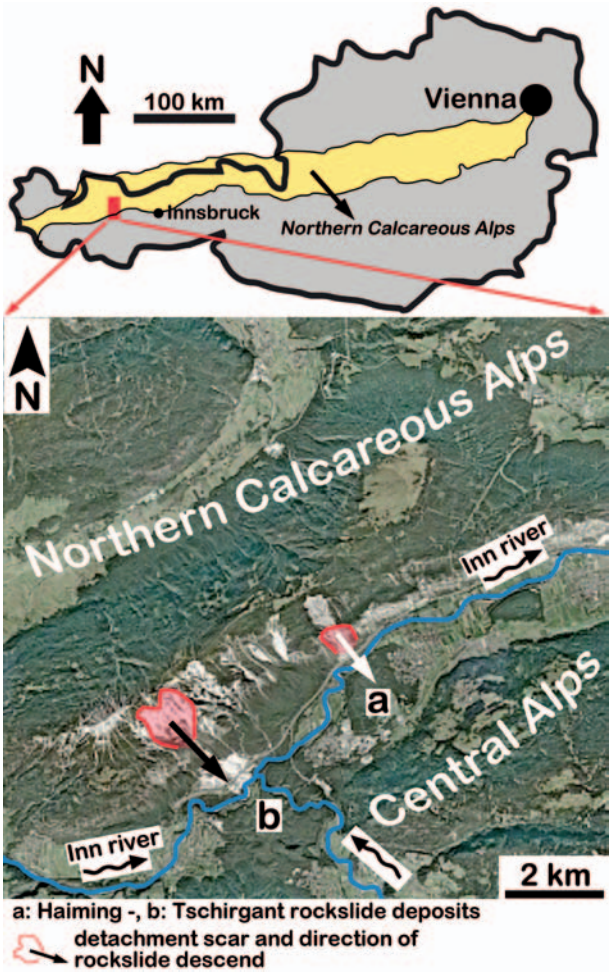

Fig. 2: Location of rock avalanches and associated scree slopes mentioned in the present paper.

lues of scree deposition, all rates were plotted in a ‚Sadler diagram' (cf. Sadler, 1981, 1999), and compared with other rates of geomorphic change in mountain ranges.

Geologic and climatic setting

The Northern Calcareous Alps (NCA) consist of stacked cover-thrust nappes mainly of Triassic shallow-water carbonate rocks (Schmid et al., 2004). Because of heteroaxial folding and brittle faulting during Alpine orogenesis, the carbonate rocks of the NCA are more-or-less densely riddled by joints and faults (Eisbacher and Brandner, 1996). During structural deformation, limestones deformed in brittle and brittle-ductile fashion; conversely, dolostones reacted brittlely and thus typically are densely jointed. As a result, in the Eastern Alps, scree shedding from dolostone cliffs typically is more intense than from cliffs of limestones (Sanders et al., 2009). Over most of their extent, the scenery of the NCA is coined by glacial-interglacial cycles. Both valley deepening and steepening/heightening of mountain flanks by glacial erosion (Van Husen, 2004; Champagnac et al., 2007; Montgomery and Korup, 2011) favoured rocksliding and talus accumulation subsequent to glacial retreat. In the Eastern Alps, down-wasting of ice streams somewhen between 21 to 19 ka was completed within a thousand years at most (Van Husen, 2004). This lead to exposure of high, glacially-weakened, bare-rocky mountain flanks, and to accumulation of alluvial fans and talus slopes in comparatively low altitudes. Today, nearly all of these fan- or talus successions are abandoned, vegetated and/or undergo erosion; active modern talus typically is situated in higher altitudes, and in different geomorphic settings (cf. Sanders and Ostermann, 2011). Over all, deglacial to late-glacial talus accumulation probably was systematically higher than at present (Sass and Wollny, 2001; Sanders and Ostermann, 2011). Increased production of scree and pebbly alluvium shortly before and after full glaciations (Van Husen, 1983), later included in the concept of ‚paraglacial' deposition (Ballantyne, 2002), is supported by observations on deglacial to post-glacial sedimentation within the Alps and their foreland (Müller, 1999; Hinderer, 2001; Sanders, 2012). During deglaciation, the Inn valley became permanently ice-free from ~17.4 kyr cal BP over most of its extent, and was reforested at about 15 ka BP (Patzelt, 1980, 1987; Van Husen, 2004). With the start of the Holocene, the upper treeline ecoline in the Alps had risen to near its present altitude, and was subject to only minor fluctuations of 100-300 m ever since (cf. Tinner and Theurillat, 2003; Nicolussi et al., 2005; Tinner and Vescovi, 2005).

In the western part of the Tyrol, the NCA abut the Ötztal-Stubai metamorphic basement of the Central Alps along the Inn valley fault zone. At the northern flank of the Inn valley, two rock avalanches are present in this area (Fig. 2). In the detachment scar of each rock avalanche, scree slopes had accumulated since mass-wasting. Aside of a few, comparatively thin stratigraphic units in tectonic slivers in the scar of the Tschirgant rock avalanche (Pagliarini, 2008), with respect to the rock avalanche masses and scree slopes mentioned herein, three stratigraphic units are relevant (see Table 1): (a) the Wetterstein Dolomite unit, overlain by (b) the Northern Alpine Raibl unit (NAR unit) which, in turn, is followed up-section by

Table 1: Stratigraphic units in the investigated area that contributed to post-rockslide talus-slope formation.

Name	Range; local thickness	Lithological characteristics	Remarks
Wetterstein Dolomite (WD) unit	Ladinian to Cordevolian; at least about 800 m thick	Light-grey to whitish to pink dolostones with vugs and cavities; internal breccias with dolospar cement	(a) Haiming rockslides composed of WD (b) Scree of WD builds post-rockslide Tschirgant talus slope
Northern Alpine Raibl unit (NAR)	Julian to Tuvalian; approximately 120-150 m thick	Variegated: (a) Grey to black dolo/lime mudstones; (b) ocre-weathering limestones and cellular dolomites; (c) thick marker bed of onco-rudstone; (d) two intervals of slates	Pertinent only for Haiming post-rockslide talus Comprises a significant part to post-rockslide talus of Haiming
Hauptdolomit unit (HD)	Norian; at least 700-800 m thick	HD: Light brown weathering coarse-crystalline dolostones; cryptmicrobial lamination; locally fracture breccias cemented by saddle dolomite	Pertinent for Haiming post-rockslide talus Comprises the majority of post-rockslide talus of Haiming

(c) the Hauptdolomit unit. We note that the carbonate rocks in the detachment scars are not more densely-jointed and faulted than the same rock types elsewhere along the Inn valley fault zone, and in other areas of more intense structural deformation of the NCA. It is rather the intersection of structural weaknesses (bedding, jointing, faulting, folding) with the local, steep mountain flanks that renders them prone to rocksliding (Pagliarini, 2008). Both the Haiming and the Tschirgant rock avalanche scar are located in a rainshadow area with comparatively low mean annual precipitation (Table 2). The mountain flank from which the Haiming rock avalanche detached is forested up to its local crestline between 1760–1800 m a.s.l. mainly by *Pinus sylvestris*, *Picea abies*, and *Juniperus communis*. In its lower part, the mountain flank laterally adjacent to the Tschirgant rock avalanche detachment scar is mantled up to about 1800 m a.s.l. by forest mainly of *P. sylvestris, P. abies* and *J. communis*; above, up to the crestline between about 2100–2200 m a.s.l., a dense cover of *Pinus mugo* and Ericaceae is locally interspersed with rock exposures. As obvious from the setting the scree slopes within, both, the Tschirgant and the Haiming rock avalanche scars have not been exploited by man before, such as for pasture or extracting wood.

Rock avalanches, talus, accumulation rates

Haiming

The mountain flank adjacent north of Haiming consists of a folded, subvertically tilted succession ranging from the Wetterstein Dolomite to the Hauptdolomit unit (see Table 1) (Figures 3A and 4). Over most of its extent, the considered mountain flank is characterized by forested, formerly active scree slopes along the toe of a laterally continuous cliff of Wetterstein Dolomite. In the detachment scar of the Haiming rock avalanches, however, the cliff is breached by a gap. At Haiming, radiocarbon dating indicates that three superposed rock avalanche masses are present. All outcrops, natural and artificial, indi-

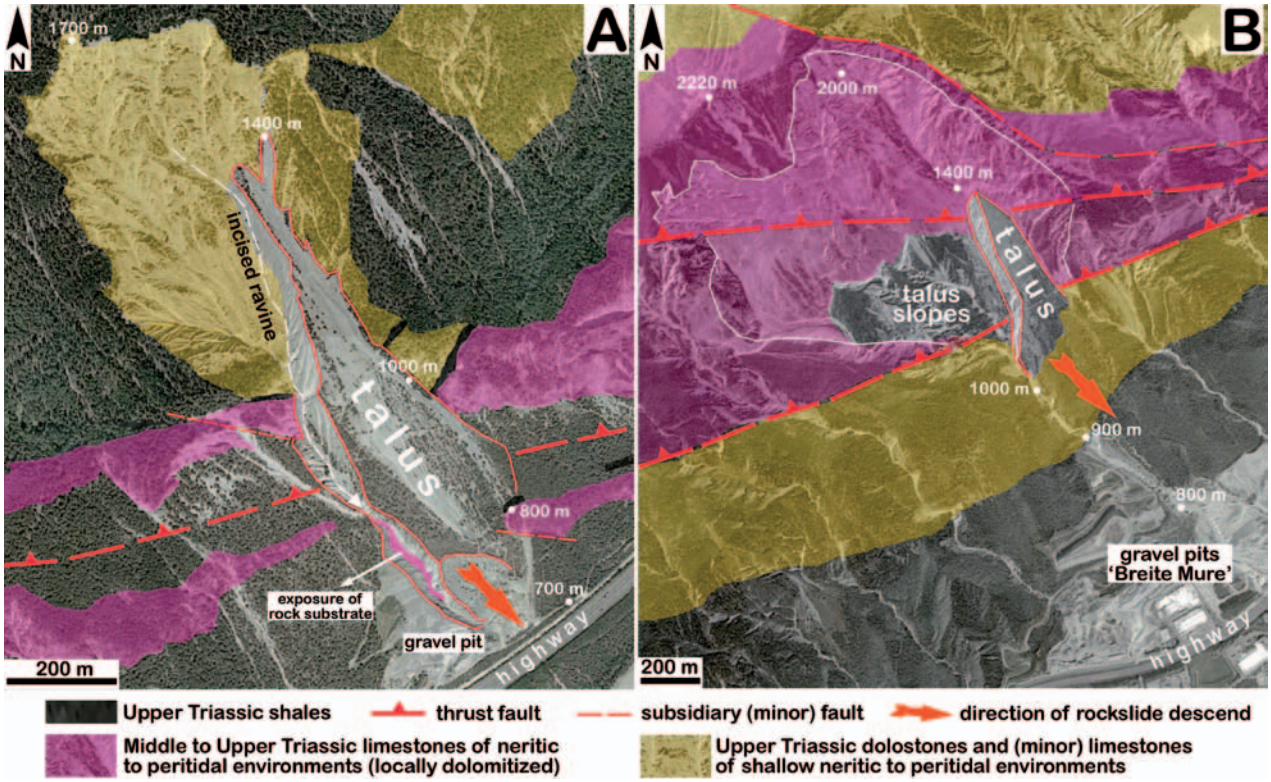

Fig. 3: Geological maps of rock avalanche scars of Haiming (A) and Tschirgant (B). A. Following the Haiming rock avalanches, a talus about 700 m in vertical amplitude accumulated. Excavation of a gravel pit resulted in complete exposure of the talus succession down to the rock substrate. B. At Tschirgant, rock avalanche descend was followed by accumulation of a large alluvial fan exploited for gravel (gravel pits ‚Breite Mure') and, higher upslope, of talus slopes. In this paper, the talus marked by the arrowtip is considered.

cate that at least the two younger rock avalanches consist exclusively of Wetterstein Dolomite. The deposit of the oldest rock avalanche ‚Haiming 1', dated to cal BC 1690-1500, is exposed only along the distalmost fringe of the rock avalanche deposits (G. Patzelt, pers. comm., 2011); this event is no longer considered herein. The intermediate rock avalanche event ‚Haiming 2' is topped by a soil with charcoal (Fig. 4). The youngest rock avalanche event ‚Haiming 3' was age-dated by the root stock of a tree that has been truncated by the overriding rock avalanche (Fig. 4); this latest event is relevant for the talus slope considered herein (Table 3). At least the rock avalanche events Haiming 2 and 3, respectively, most probably detached from the subvertically-tilted intervals of shales of the NAR unit, combined with a system of steeply south-dipping faults and joints (Fig. 4). Today, the scar produced by rocksliding is crossed-over by an active talus slope. Because the rock avalanche masses consist of Wetterstein Dolomite, the upper part of the cliff consisting of NAR unit and, mainly, of Hauptdolomit probably formed by retrogressive erosion and slope decline after rocksliding. In its distal part, the talus was pitted for gravel from the 1970s to the 1990s. Scree exploitation led to exposure of the complete talus succession down to the rock substrate; in addition, the lowering of local base-level by pitting led to deepening of a ravine, exposing the thickness of the talus also in its proximal part. The talus succession consists practically entirely, and from bottom to top, of lithoclasts derived from the NAR unit and the Hauptdolomit unit (cf. Table 1). The Haiming rock avalanche scar degraded by slope decline while talus accumulated. The longitudinal section (Fig. 4) suggests that, in absence of local base-level lowering by gravel pitting, the cliff/talus system would soon have reached a stage where an inclined rocky slope is veneered by scree, and further retreat is terminated or extremely slow. Both, the position of the talus across the rock avalanche scars and its lithological composition indicate that it accumulated

Table II: Data of meteorological stations ‚Haiming' and ‚Imst' adjacent to the rockslides mentioned in the present paper, and comparative data from lower- and higher-located stations. Selection of the other stations was made to cover an altitude range up to more than 3000 m a.s.l. Measurement interval 1971-2000. Data source: www.zamg.ac.at, except for Holdridge (1947) mean annual biotemperatures and biomes. See text for discussion.

Station, altitude, position	Kirchbichl, 498 m a.s.l. (12°5'/47°31')	Haiming, 695 m a.s.l. (10°51'/47°15')	Imst, 910 m a.s.l. (10°44'/47°14')	St. Anton am Arlberg, 1298 m a.s.l. (10°16'/47°8')	Galtür, 1583 m a.s.l. (10°11'/46°58')	Obergurgl, 1938 m a.s.l. (11°2'/46°52')	Obergurgl, 1938 m a.s.l. (11°2'/46°52')	Obervermunt, 2040 m a.s.l. (10°5'/46°55')	Patscherkofel, 2247 m a.s.l (11°28'/47°13')	Sonnblick, 3105 m a.s.l. (12°57'/47°3')
FTD	90	130	111	131	134	128	128	125	88	71
ID	21.4	17.1	22.5	38.8	59.6	68.4	68.4	85.2	134.6	239
MAAT (°C)	8.0	7.4	7.0	4.5	2.7	2.2	2.2	1.3	0.0	–5.5
MBT (°C)	8.3 (montane, wet forest)	7.9 (montane, moist forest)	7.5 (montane, moist forest)	4.75 (subalpine, rain forest)	4.3 (subalpine, rain forest)	3.7 (subalpine, rain tundra)	3.7 (subalpine, rain tundra)	3.2 (subalpine, rain tundra)	2.5 (alpine, rain tundra)	0.37 (nival)
MAP (mm)	1135	717	799	1275	1128	819	819	1109	879	1673
MHMP (mm)	158 (july)	110 (july)	117 (august)	162 (july, august)	156 (july)	91 (july)	91 (july)	189 (july)	132 (july)	164 (june)
MPR24 (mm)	82 (july)	97 (may)	85 (may)	75 (may)	75 (august)	70 (july)	70 (july)	69 (august)	72 (august)	–
Altitude of apex of nearest active scree slopes	NCA, Kaisergebirge, east of Kirchbichl: 1550-1650m a.s.l.	NCA, Apices of scree slopes along the mountain crest that shed the rock avalanches: 1400-1500 m a.s.l. Northern part of Ötztal basement: 2200-2400 m a.s.l.	NCA northwest of Imst: 2100-2400 m a.s.l.	NCA north of St. Anton: 1900-2500 m a.s.l.	Range north of Galtür: 2400-2600 m a.s.l.	SE of Obergurgl: 2500-2700 m a.s.l.	SE of Obergurgl: 2500-2700 m a.s.l.	Environs of Obervermunt: 2450-2600 m a.s.l.	Apices of small scree slopes up from c. 2000 m a.s.l. (deep-seated, slow gravitational deformation)	N slope of Sommblick massif: 2400-2700 m a.s.l.

Key:
FTD = Freeze-thaw days; mean annual number of days with air-temperature changing from <0°C to >0°C
ID = Ice days; mean annual number of days with air-temperature staying < 1°C
MAAT = Mean annual air temperature
MBT = Holdridge (1947) mean annual biotemperature, with biome designation
MAP = Mean annual precipitation
MHMP = Mean of highest monthly precipitation per year (with month)
MPR24 = Maximum precipitation as rain per 24 h (with month)

Holdridge (1947) MBT is calculated as sum of all ‚growing months' with a mean temperature Tg in the range of 0 < Tg < 30°C, divided by 12.
Months with a mean temperature of ≤0°C are included as zero.
So: MBT = Σ Tg/12
note to row ‚Presence of nearest active scree slopes': Herein, the approximate altitude of the apex of the nearest active scree slopes is listed. Ephemerally waterrun ravines located in otherwise vegetated terrain are not considered as active scree slopes.

after descend of the younger rock avalanche ‚Haiming 3' (Table 3).

Tschirgant

At Tschirgant, two different suites of radiocarbon ages indicate that the rock avalanche mass results from superposition of two mass-wasting events separated by about 600 years (Table 3) (Prager et al., 2008); this is supported by U/Th ages of soda-straw stalactites formed underneath rock avalanche boulders (Ostermann and Sanders, 2010). The detachment scar of the Tschirgant rock avalanches is cut into a folded and faulted, subvertically-tilted, Middle to Upper Triassic succession of dolostones and, subordinately, of cellular dolomites and limestones (Fig. 3B) (Pagliarini, 2008). The main part of the detachment scar, however, is cut into the Wetterstein Dolomite (cf. Table 1). The lithological succession as arranged in the detachment scar overall is retained within the Tschirgant rock avalanche mass, except for minor foldings and thrustings (Patzelt and Poscher, 1993). Because the medial and proximal part of the composite rock avalanche mass consists only of Wetterstein Dolomite, it seems probable that the younger rock avalanche detached upslope of about 1350-1400 m a.s.l., where Wetterstein Dolomite is exposed (Fig. 3B). Subsequent to rocksliding, a large alluvial fan (‚Breite Mure') formed beyond the toe of the scar; in addition, talus slopes accumulated within the detachment scar. Field inspection and satellite orthoimages suggest that two generations of talus are present: An apparently older generation of talus slopes occupies the western part of the scar; these slopes are vegetated by P. mugo and are erosionally incised. In contrast, the eastern part of the scar is floored by a talus with unvegetated surface (Fig. 3B); this talus may be younger and post-date the second rock avalanche event. Because of its good exposure, the thickness of the eastern talus slope was determined by geometrical construction from isohypsed satellite orthoimages on a scale of 1/1000. Dividing the thickness of the scree slopes in the detachment scars by the rock avalanche event age yields a mean accumulation rate of talus (Table 3). For the Tschirgant location, two ranges of mean talus accumulation rates were calculated (see above). The present detachment scar of the Tschirgant rock avalanches still towers hundreds of meters high, yet even the eastern talus considered herein (Fig. 3B) has attained a state of low activity and, probably, of scree supply from the cliff above; in case of the Tschirgant scar, this lowering of scree production can not be explained by autocyclic fade-out due to cliff burial (see below for discussion).

Accumulation rates

The mean accumulation rates of the Haiming and Tschirgant talus slopes are compared by a Sadler plot with rates deduced from data of other authors (Fig. 5). Sadler (1981) had demonstrated that all sedimentary deposits are subject to a systematic negative correlation between accumulation rate and the corresponding time interval of consideration: in other words, the longer the considered time interval, the lower is the accumulation rate (see also Anders et al., 1987). A similar inverse correlation holds also for rates of erosion versus time interval of consideration (Gardner et al., 1987). To compare just sedimentation/erosion rates without their corresponding time interval of consideration thus at best is hazardous, and can lead to spurious results (see, e. g., Sadler, 1999; Willenbring and von Blanckenburg, 2010). Another advantage of a Sadler plot is that it allows for estimates from a limited set of accumulation rates towards longer and shorter time intervals. The rate data plotted in Figure 5 indicate the universal, inverse ‚Sadler correlation' of accumulation rate with time span.

Interpretation and discussion

Sadler plot

As the Sadler plot (Fig. 5) implies, the comparatively high mean accumulation rates of the Haiming and Tschirgant talus slopes (Table 3) indicate that the initial rate of scree deposition shortly after detachment of the rock avalanches was much higher, but then shrinked to lower rates. In the Alps, the detachment scars of practically all rockslides and rock avalanches contain scree slopes. Also the scars of young historical rock avalanches are decorated with scree slopes; the scar of the 1908 Frank slide (Rocky Mountains) contains a large talus apron. The scar of the 1987 rock avalanche of Bormio (Southern Alps) also contains scree slopes that, to judge from their extent, may be some 10 m or more in thickness in their

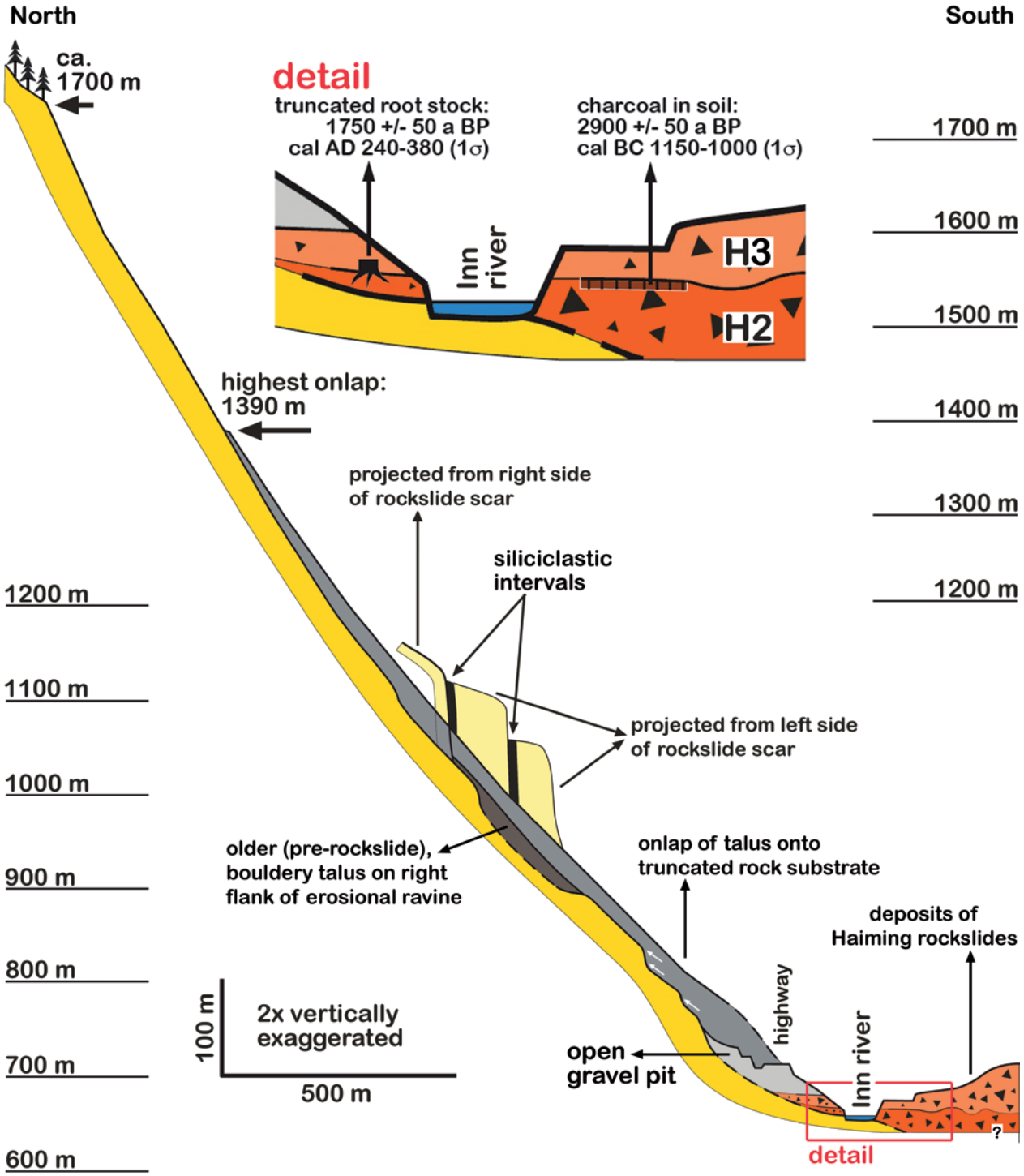

Fig. 4: Section along the talus and the proximal part of the combined Haiming rock avalanche masses (cf. Fig. 2). At least the two rock avalanches H2 and H3 (see text) probably detached from sub-vertically tilted interval of shales, combined with steeply south-dipping to subvertical joint- and fault surfaces (not shown). Closely north and south of the Inn river, two rock avalanche events H2 and H3 can be distinguished (see inset detail, and Table 3). Subsequent to the younger rock avalanche event H3 (cal AD 380-240), a large talus slope accumulated.

Age data kindly provided by Gernot Patzelt.

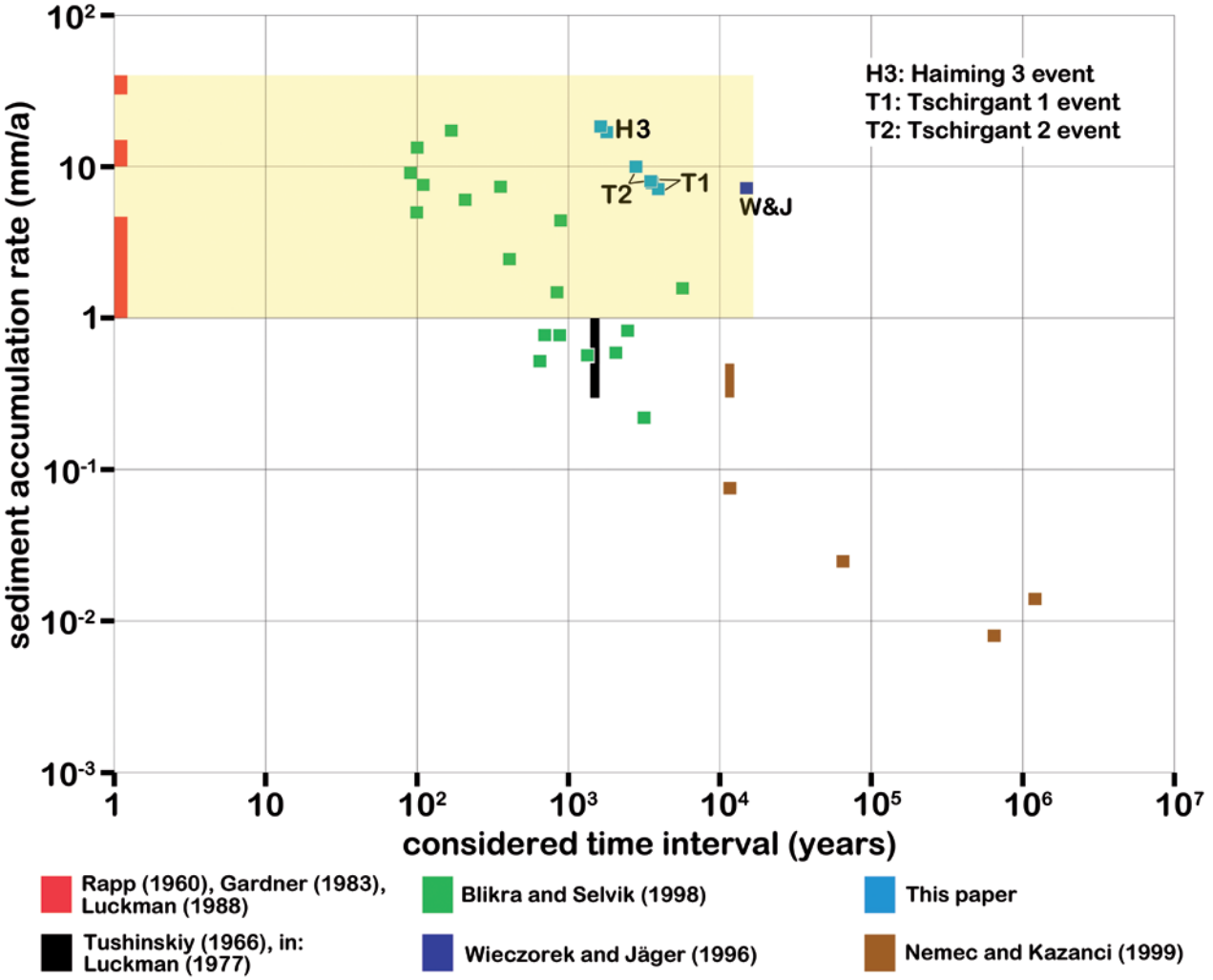

Fig. 5: Plot of sediment accumulation rate (y-axis) as a function of considered time interval of accumulation (x-axis) (‚Sadler plot', see text). The light-yellow field is delimited at its base and top by annual scree accumulation rates in temperate to subarctic mountain ranges. Note: (a) inverse correlation of accumulation rates with time interval, (b) within the light-yellow field, the range of accumulation rates over four orders of magnitude of time interval.

distal part. If cliff retreat is seen as a proxy for scree production, this implies that immediately after new exposure of cliffs by mass-wasting, the cliffs retreat at very high pace. After mass-wasting, the newly-defaced cliffs certainly were rich in loosened rock material supplying much more scree than a cliff exposed for thousands of years (see discussion below).

The mean accumulation rates of the Haiming and Tschirgant talus slopes are one to two orders of magnitude higher than rates in corresponding time intervals of Blikra and Selvik (1998), but lower than the rates deduced from data in Wieczorek and Jäger (1996). The ^{14}C ages of Blikra and Selvik (1998) that provide the base for the rates in Figure 5 are mainly from soils intercalated into talus successions. Thus, the ‚real' accumulation rates of talus intervals in between the soils were higher, and talus accumulation times were shorter by an unknown amount. In the Sadler plot, this implies that the ‚real' talus accumulation rates for the data of Blikra and Selvik (1998) would shift towards the upper left. There is, however, no way to correct the error, so the data had to be plotted in the way as shown. The scree slopes investigated by Blikra and Selvik (1998) are supplied from gneiss terrains, a rock type considered to disintegrate slower than deformed carbonate rocks (e.g., André, 1997). The scree slopes described in Wieczorek and Jäger (1996) are supplied from the granitic to gra-

nodioritic cliffs of Yosemite valley. Estimating total talus volume since the last deglaciation (15 ka BP) in Yosemite valley, Wieczorek and Jäger (1996, p. 29, and their Fig. 10) arrived at thickness estimates for individual slopes of 100-120 m; this transfers to a mean accumulation rate of 6.7 mm/a (100 m thick talus) to 8 mm/a (120 m thick talus) over the past 15 ka (Fig. 5). Lithology indeed seems to be of minor importance with respect to long-term talus accumulation; rather, local topographic relief, structural disintegration (faulting, jointing), slope dip and climate appear to be significant (Hales and Roering, 2005; cf. Norton et al., 2010). Overall, thus, the accumulation rates of the Haiming and Tschirgant talus slopes appear as high, but not outrageous. Most notable, however, is that the long-term accumulation rates in the light-yellow field in Figure 5 overlap with annual accumulation rates of scree in temperate to subarctic mountain ranges. Following the inverse Sadler correlation, projecting the calculated mean rates upwards towards the one-year ordinate, this suggests that short-term rates of scree accumulation may attain up to about one meter or more per year.

Most documented rates of cliff retreat of temperate to subarctic mountain ranges overlap with rates of retreat of semi-arid to hyper-arid regions; only a few, but largely conjectural, retreat rates of subaerial cliffs in subarctic settings are much higher (Fig. 6). The similarity of retreat rates from highly different climatic settings may be interpreted in two ways. (1) Cliff retreat in temperate and subarctic mountain ranges is still too little documented, such that higher rates remain to be demonstrated. (2) A combination of processes other than frost-related weathering, such as thermal stress fatigue, subcritical joint growth, rainwash, snow avalanches, exfoliation, and phases of increased joint-water pressure can also be highly effective in cliff erosion (see, e. g., Wieczorek and Jäger, 1996; Hall, 1999; André. 2003; Hall and André, 2003; Wieczorek et al., 2008; Matasci et al., 2011; Krautblatter and Dikau, 2007).

Processes of scree production

Frost cracking is generally considered significant in producing scree from intact rock. Frost weathering works by growth – within a specific range of cooling rates – of segregation ice between about -3 to -8°C (‚frost-cracking window'; e. g., Walder and Hallet, 1985, 1986; Hallet et al., 1991; Matsuoka, 2001; Murton et al., 2006), although slightly different subzero temperature ranges are locally indicated (Matsuoka, 2001; Anderson & Anderson, 2010). Beyond this, one may distinguish two ‚schools': School (a) favouring frost cracking by segregation ice growth during the annual frost cycle; this school chiefly relies on physical models and extrapolation of experiments (Walder and Hallet, 1985, 1986; Anderson, 1998; Murton et al., 2001, 2006; Anderson & Anderson, 2010). School (b) acknowledges the significance of the annual frost cycle (Matsuoka and Sakai, 1999), but mainly provides field evidence and in-situ field measurements showing that the diurnal cycle can be at least as important as or even override the annual cycle (Matusoka et al., 1997; Matsuoka, 2001; Hall, 2004; Matsuoka and Murton, 2008; Robinson and Moses, 2011). The latter implies that it is difficult to place a lower altitude limit to the production of scree by frost cracking because, either, the annual and/or the diurnal freeze-thaw cycles may be effective. Conversely, the upper limit of scree production by frost cracking is near the lower limit of continuous permafrost. Even in altitudes with continuous permafrost, and even at subzero temperatures, however, rockfalls can spall off due to weakening (not melting!) of permafrost ice at subzero temperatures (Davies et al., 2001; Nötzli and Gruber, 2005). Over all, however, the lower limit of continuous permafrost can be considered as a proxy for the upper altitude limit of frost-related scree production. In the absence of long-term, in-situ temperature/humidity measurements from the detachment scars of the rock avalanches (compare Coutard and Francou, 1989; Hall, 2004), for sake of comparison, I used records from meteorological stations (Table 2). One may rebut the use of meteodata by pledging the complexity, in time and space, of frost-related weathering. Yet the mere view on mountain ranges shows that scree slopes prevail within, but are not confined to, a specific altitude range. The prevalence of scree slopes in a specific altitude span is explained by Hales and Roering (2005, 2009) as that range wherein the annual number of days with temperatures within the frost-cracking window is maximum. They did this not by placing hundreds of in-situ loggers into cliffs, but by large-scale analyses of mean annual air temperature with altitude, compared to the altitude distribution of active scree slopes. For if the concept of maximum frost-related weathering within a certain altitude range (and, by implication, yearly temperature range) is true at all, to explain the large-scale distribution of active scree slopes, their approach seems methodically correct. So, for sake of a gross comparison with other locations in the Alps, the use of meteodata is justified.

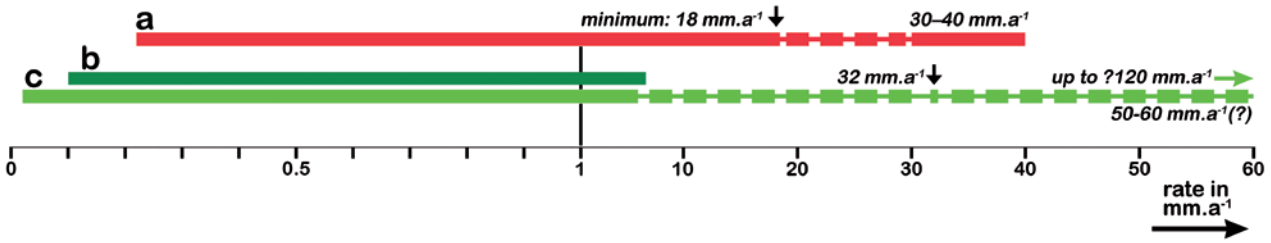

Fig. 6: Bar plot of rates of: (a) talus accumulation, (b) cliff retreat in semi-arid to hyper-arid areas, and (c) cliff retreat in temperate to sub-arctic areas. Note lateral change in scale at rate 1 mm/a. Ranges covered by most documented rates indicated as solid bars; outlier values are indicated separately. Rates of cliff retreat of 50-60 mm/a or 120 mm/a above subarctic rock glaciers are crude estimates only (Humlum, 2000). Rates of talus accumulation from: Blikra and Selvik (1998), Gardner (1983), Luckman (1988), Nemec and Kazanci (1999), Tushinskiy (1966) (cit. in Luckman, 1977, p. 36), Wieczorek and Jäger (1996). Rates of cliff retreat from: André (1997), André (2003), Barsch (1996), Delmas et al. (2003), Gerson (1982), Gutiérrez et al. (1998), Hales and Roering (2009), Heimsath and McGlynn (2008), Hétu and Gray (2000), Humlum (2000), Matsuoka (2008), Rapp (1960), Sass and Wollny (2001), Sass (2010), Seong et al. (2009). Note1: Several of the cited papers for rates of cliff retreat contain compilations of previous works that were implicitly included into the bar diagrams. Note 2: Because of highly different methods and different time intervals of observations used to deduce erosion rates of cliffs, comparison of rates of talus accumulation with retreat rates of cliffs in a simple bar diagram was preferred. Because the bar diagram is a mere comparison of rates without time interval of observation, the comparability of these datasets is limited. See text for discussion.

From Table 2, I read the following features: (1) In the altitude range from the stations Haiming (695 m a.s.l.) to Obervermunt (2040 m a.s.l.), the mean annual number of freeze-thaw days (FTD) does not markedly change, and does not show a specific trend. Only for stations still higher up, the number of FTD decreases significantly. In the Alps, thus, a comparatively high annual number of air-FTD (see Hales and Roering, 2005) ranges over about 1500 m in altitude. This fits the general observation that temperate mountain ranges show a high number of FTD per year, because freeze-thaw cycling distributes over different seasons in different altitudes (French, 2007). (2) Up from station Haiming, the mean annual number of ice days (ID) steadily increases with altitude, while mean annual air temperature (MAAT) decreases, as does the Holdridge (1947) mean annual biotemperature (MBT). (3) All of the parameters for precipitation (MAP, MHMP, MPR24; see Table 2) do not show a single trend with altitude; this is related to regional variations in precipitation regime. With respect to MAP and MHMP, the stations Haiming and Imst show low relative values. Only with respect to MPR24, both these stations are located at the upper end of the range, but do not substantially exceed the values of other stations. (4) It is clear that the altitudes of the apices of active scree slopes (=toe line of cliffs; see Table 2) near each meteostation are controlled by an interplay of geological, geomorphological and climatic factors. Nevertheless, they provide an idea at which gross altitude rock cliffs are located that shed enough scree to sustain active scree slopes. The apices of scree slopes in the NCA are typically located between ~1800–2200 m.a.l. (Angermaier, 2011), i. e. lower than those of the Central Alps (Table 2). This most probably results from a combination of geological controls (faulting, jointing) and morphology. In the NCA, glacial erosion during the LGM to late-glacial interval produced deep, steeply-incised cirques bounded by cliffs that shed scree at comparatively low altitudes. In addition, structural disintegration of rocks is crucial: Along the mountain range between the Haiming and Tschirgant rock avalanches, the apices of scree slopes that are not associated with defacing by post-LGM mass-wasting are located between 1400-1500 m a.s.l.; this is a low altitude relative to most other locations (see Table 2). Conversely, a few kilometers to the south, along the northernmost fringe of the Oetztal basement, the apices of scree slopes are located between 2200-2400 m.

All in all, I see no obvious or strict correlation between: number of ice days (ID) and number of freeze-thaw days (FTD) with presence/absence and altitude range of scree slopes, up to lower terminations of glaciers (e. g. near station Sonnblick). This may be explained by several factors. (a) The topographic altitude of cliff toes, and the vertical height of cliffs, were largely produced by erosion during full glaciations. In the Central Alps, trimlines of the LGM were generally higher-positioned than in the NCA (see Van Husen, 1987). In the NCA, today, practically all cirques are devoid of ice. Many of these cirques were shaped by glacial incision during the LGM to late-glacial (and perhaps during earlier glaciations; H. Kerschner, pers. comm.). (b) Diurnal freeze-thaw cycling, and rock cracking by growth of segregation ice during

the annual frost cycle, may both be similarly effective in producing scree, compensating each other over a large span of altitude. This may help to explain the presence of scree-slope apices over an altitude range of more than 1.2 kilometer (Table 2). (c) Finally, the combined effects of processes related to rain, snow and ‚dry' temperature cycling may be similarly effective in liberating scree from cliffs than is frost-related weathering. Relative to the large research effort invested since decades into frost weathering, however, to date the roles of ‚non-cold processes' in cliff erosion and scree accumulation are only scarcely explored (André, 2003). At least in cliffs of faulted and jointed carbonate rocks, rainfall is a major factor in supplying scree to talus; furthermore, hydrostatic pressure in fractures or along bedding planes and schistosity can trigger rockfalls even well-after rain (Krautblatter and Dikau, 2007).

Significance of vegetation

Between 380 A.D. to 2050 B.C., the upper treeline ecoline in the Eastern Alps was located between about 2150–2280 m a.s.l. (Nicolussi et al., 2005); the mountain flank from which the two rock avalanches detached thus were covered by forest, similar to its present status. Scree production subsequent to rock avalanching proceeded: (a) in an altitude range vegetated for thousands of years before, and (b) in an interglacial climate well-after deglaciation. This seems to contradict a concept of scree production and vertical distribution of active scree slopes based chiefly on the annual frost cycle.

I suggest that the prevalence of active scree slopes in a certain altitude range is chiefly related to post-glacial climb of vegetation (cf. Table 2), superposed with the altitude range of all processes that can produce scree from cliffs. In this interpretation, the concept of the ‚frost-cracking window' remains valid, yet frost cracking is just one of several important processes to liberate rock fragments from cliffs. This interpretation implies that rocky slopes that potentially could shed scree may be shut off talus production by being vegetated. In the NCA, cliffs hundreds of meters in height became stripped of vegetation and soil by wildfires; this resulted in bare-rocky cliffs (termed ‚Plaike' in German) intercalated between forested mountain flanks of identical steepness. For instance, Arnspitz Plaike near Innsbruck, formed in 1946, still is only patchily colonized by grasses, Ericaceae, and *Primula auricula* (Sass et al., 2006). Three talus fans along the toe of the Plaike have significantly gained in volume and activity, and ‚diffuse' downslope debris-transport by snow avalanches has increased, since stripping of vegetation (Sass et al., 2006; Sass et al., 2010). These observations underscore the role of vegetation in long-term dynamics and distribution of active scree slopes.

Conclusions

(1)
In the Eastern Alps, active scree slopes within the detachment scars of two late Holocene rock avalanches had accumulated at mean rates of 7–18 mm/a over time spans of about 1.7–3.8 ka. The rock cliffs (detachment scars) that shed the scree extend from ~900–1700 m a.s.l. (Haiming) and from ~900–2100 m a.s.l. (Tschirgant). At the time of rock avalanching, the mountain flank laterally adjacent to the scree slopes was forested, as it is today.

(2)
A ‚Sadler plot' (= accumulation rate as a function of time interval) implies that the mean accumulation rates of the talus in the detachment scars are high, but not exceedingly higher than mean accumulation rates of other scree-slope successions. Furthermore, the ‚Sadler plot' suggests that the rate of scree deposition was much higher early after rock avalanching, and then diminished.

(3) The two talus slopes are located at much lower altitudes than most other scree slopes of the Eastern Alps. A comparison of meteorological data (1971-2000) from stations ranging from 498 to 3105 m a.s.l. suggests that the intense scree production is hardly explained by the annual number of ice days (IC; days with $T < 0°C$); the annual number of freeze-thaw days (FTD), in contrast, remains nearly constant from station Haiming (695 m a.s.l.) up to Obervermunt (2040 m a.s.l.). Thus, talus production may be mainly controlled by FTD or by, both, FTD and ID compensating each other with increasing altitude. In addition, processes unrelated to frost probably signficantly contribute to scree production, such as ‚scraping' off scree by heavy rainfalls and snow cascading/avalanching down cliffs, spalling of rock by increased pore-water pressure, and rock cracking by thermal stress fatigue well-above the freezing point.

(4)
As mentioned, the two talus slopes accumulated in between mountain slopes that were forested at the time of rock avalanching, and at much lower altitude than

Table III: Event ages of rockslides, and calculated mean rates of talus accumulation.

Rockslide event	Mean event age(s)	Reference for age	Mean talus accumulation rates
Haiming 3	cal AD 380-240	Figure 4 (Patzelt, pers. comm.)	17 - 18.4 mm/a (for 30 m talus thickness)
Tschirgant 1	3735 ± 125 3785 ± 105 3740 ± 100 combined mean: **3753 ± 191 cal yrs BP**	Prager et al. (2008, p. 400)	7.1 - 7.9 mm/a (for 28 m talus thickness)
Tschirgant 2	3470 ± 220 2975 ± 275 3010 ± 70 2505 ± 175 combined mean: **3151 ± 359 cal yrs BP**	Prager et al. (2008, p. 400)	8 - 10 mm/a (for 28 m talus thickness)

most other scree slopes of the Eastern Alps. I suggest that the prevalence of presently active scree slopes in a certain altitude range (~1800 to ~2600 m a.s.l.) of the Eastern Alps results from: (a) the overall morphology and altitude of the orogen, (b) medium-scale morphology produced mainly by glacial erosion, (c) post-glacial climb of vegetation, superposed with (d) an optimal combination of all processes (irrespective of their altitude range) capable to liberate scree from cliffs, and at a combined rate high enough to sustain a sizeable, active scree slope. This interpretation does not invalidate but embeds the concept of the ‚frost-cracking window'. The role of vegetation cover in influencing scree production from steep, rocky mountain flanks (technically cliffs up from slope dip ≥45°) has been underestimated.

Acknowledgements

Gernot Patzelt (former Institute of High-Alpine Research, University of Innsbruck) is thanked for kindly providing his radio-carbonages and detailed discussions of numerical ages and rock avalanche stratigraphies. Ulrich Swoboda, Intergeo, and ASFINAG Alpenstrassen AG, provided drill logs of the Haiming talus. Brigitta Erschbamer (Institute of Botany, University of Innsbruck) adviced in calculation of Holdridge biotemperatures. Christoph Prager, alpS–Centre of Alpine Hazard Management, Innsbruck, and an anonymous reviewer are thanked for constructive comments.

References

Anders, M.H., Krueger, S.W. and Sadler, P.M. (1987): A new look at sedimentation rates and the completeness of the stratigraphic record. – Journal of Geology, 95: 1-14.

Anderson, R.S. (1998): Near-surface thermal profiles in alpine bedrock: implications for the frost weathering of rock. – Arctic and Alpine Research, 30: 362–372.

Anderson, R.S. and Anderson, S.P. (2010): Geomorphology. The mechanics and chemistry of landscapes. – Cambridge University Press, Cambridge, 637 pp.

André, M.-F. (1997): Holocene rockwall retreat in Svalbard: a triple-rate evolution. – Earth Surface Processes and Landforms, 22: 423-440.

André, M.-F. (2003): Do periglacial landscapes evolve under periglacial conditions? – Geomorphology, 52: 149-164.

Angermaier, J. (2011): Felswandhöhe gegen Schutthalden-Höhen, Nördliche Kalkalpen: Gibt es systematische Zusammenhänge? – Unpubl. BSc thesis, Univ. of Innsbruck, 56 pp.

Ballantyne, C.K. (2002): Paraglacial geomorphology. – Quaternary Science Reviews, 21: 1935-2017.

Barsch, D. (1996): Rock glaciers. Indicators for the present and former geoecology in high mountain environments. – Springer, Berlin, 331 pp.

Blikra, L. and Selvik, S.F. (1998): Climatic signals recorded in snow avalanche-dominated colluvium in western Norway: depositional facies successions and pollen records. – The Holocene, 8: 631-658.

Champagnac, J.D., Molnar, P., Anderson, R.S., Sue, C., and Delacou, B. (2007): Quaternary erosion-induced isostatic rebound in the western Alps. – Geology, 35: 195-198.

Clowes, A. and Comfort, P. (1987): Process and Landform: An outline of contemporary geomorphology. – Oliver & Boyd, Edinburgh, 335 pp.

Coutard, J.-P. and Francou, B. (1989): Rock temperature measurements in two alpine environments: Implications for frost shattering. – Arctic and Alpine Research, 21: 399-416.

Davies, M.C.R., Hamza, O., and Harris, C. (2001): The effect of rise in mean annual temperature on the stability of rock slopes containing ice-filled discontinuities. – Permafrost and Periglacial Processes, 12: 137-144.

Delmas, M., Calvet, M. and Gunnell, Y. (2009): Variability of Quaternary glacial erosion rates - a global perspective with special reference to the Eastern Pyrenees. – Quaternary Science Reviews, 28: 484-498.

Eisbacher, G.H. and Brandner, R. (1996): Superposed fold-thrust structures and high-angle faults, Northwestern Calcareous Alps, Austria. – Eclogae geologicae Helvetiae, 89: 553-572.

Erismann, T.H. and Abele, G. (2001): Dynamics of rock avalanches and rockfalls. – Springer, Berlin, 316 pp.

Evans, S.G., Scarascia Mugnozza, G., Strom, A.I., Hermanns, R.L., Ischuk, A. and Vinnichenko, S. (2006): Landslides from massive rock slope failure and associated phenomena. – In: Evans, S.G., Scarascia Mugnozza, G., Strom, A. and Hermanns, R.L. (eds.), Landslides from massive rock slope failure. NATO Science Series, Springer, Dordrecht, pp. 3-52.

French, H.M. (2007): The periglacial environment. – John Wiley & Sons Ltd, Chichester, 458 pp.

Gardner, J.S. (1983): Observations on erosion by wet snow avalanches, Mount Rae area, Alberta, Canada. – Arctic and Alpine Research, 15: 271-274.

Gardner, T.W., Jorgensen, D.W., Shuman, C. and Lemieux, C.R. (1987): Geomorphic and tectonic process rates: Effects of measured time interval. – Geology, 15: 259–261.

Gerson, R. (1982): Talus relicts in deserts: A key to major climatic fluctuations. – Israel Journal of Earth Sciences, 31: 123-132.

Gutiérrez, M., Sancho, C. and Arauzo, T. (1998): Scarp retreat rates in semiarid environments from talus flatirons (Ebro Basin, NE Spain). – Geomorphology, 25: 111-121.

Hales, T.C. and Roering, J.J. (2005): Climate-controlled variations in scree production, Southern Alps, New Zealand. – Geology, 33: 701-704.

Hales, T.C. and Roering, J.J. (2009): A frost „buzzsaw" mechanism for erosion of the eastern Southern Alps, New Zealand. – Geomorphology, 107: 241-253.

Hall, K. (1999): The role of thermal stress fatigue in the breakdown of rock in cold regions. – Geomorphology, 31: 47-63.

Hall, K. (2004): Evidence for freeze-thaw events and their implications for rock weathering in northern Canada. – Earth Surface Processes and Landforms, 29: 43-57.

Hall, K. and André, M.-F. (2003): Rock thermal data at the grain scale: Applicability to granular disintegration in cold environments. – Earth Surface Processes and Landforms, 28: 823-836.

Hallet, B., Walder, J.S. and Stubbs, C.W. (1991): Weathering by segregation ice growth in microcracks at sustained sub-zero temperatures: Verification from an experimental study using acoustic emissions. – Permafrost and Periglacial Processes, 2: 283-300.

Heimsath, A.M. and McGlynn, R. (2008): Quantifying periglacial erosion in the Nepal high Himalaya. – Geomorphology, 97: 5-23.

Hétu, B. and Gray, J.T. (2000): Effects of environmental change on scree slope development throughout the postglacial period in the Chic-Choc Mountains in the northern Gaspé Peninsula, Québec. – Geomorphology, 32: 335-355.

Hinderer, M. (2001): Late Quaternary denudation of the Alps, valley and lake fillings and modern river loads. – Geodinamica Acta, 14: 231-263.

Holdridge, L. R. (1947): Determination of world plant formations from simple climatic data. – Science, 105: 367-368.

Humlum, O. (2000): The geomorphic significance of rock glaciers: estimates of rock glacier debris volumes and headwall recession rates. – Geomorphology, 35: 41-67.

Hutchinson, J.N. (1998): A small-scale field check on the Fisher-Lehmann and Bakker-Le Heux cliff degradation models. – Earth Surface Processes and Landforms, 23: 913-926.

Ivy-Ochs, S., Heuberger, H., Kubik, P.W., Kerschner, H., Bonani, G., Frank, M. and Schlüchter, C. (1998): The age of the Köfels event. Relative, 14C and cosmogenic isotope dating of an early Holocene landslide in the Central Alps (Tyrol, Austria). – Zeitschrift für Gletscherkunde und Glazialgeologie, 34: 57-68.

Konrad, F. (2010): Mittelfristige (jahrzehntelange) Veränderungen auf karbonat-lithoklastischen Schutthalden Tirols: ein Vergleich von Luftphotos mit Satellitenphotos. – Unpubl. BSc thesis, Univ. of Innsbruck, 61 pp.

Krautblatter, M. and Dikau, R. (2007): Towards a uniform concept for the comparison and extrapolation of rockwall retreat and rockfall supply. – Geografiska Annaler, 89A: 21-40.

Luckman, B.H. (1977): The geomorphic activity of snow avalanches. – Geografiska Annaler, 59A. 31-48.

Luckman, B.H. (1988): Debris accumulation patterns on talus slopes in Surprise Valley, Alberta. – Géographie physique et Quaternaire, 42: 247-278.

Matasci, B., Stock, G.M., Jaboyedoff, M., Carrea, D., Oppikofer, T. and Pedrazzini, A. (2011): Toward an accurate detection of rockfall sources in Yosemite valley. – Geophysical Research Abstracts: EGU2011-1671.

Matsuoka, N. (2001): Direct observation of frost wedging in Alpine bedrock. – Earth Surface Processes and Landforms, 26: 601-614.

Matsuoka, N. (2008): Frost weathering and rockwall erosion in the southeastern Swiss Alps: Long-term (1994-2006) observations. – Geomorphology, 99: 353-368.

Matsuoka, N., Hirakawa, K., Watanabe, T. and Moriwaki, K. (1997): Monitoring of periglacial slope processes in the Swiss Alps: the first two years of frost shattering, heave and creep. – Permafrost and Periglacial Processes, 8: 155–177.

Matsuoka, N. and Sakai, H. (1999): Rockfall activity from an alpine cliff during thawing periods. – Geomorphology, 28: 309-328.

Matsuoka, N. and Murton, J. (2008): Frost weathering: Recent advances and future directions. – Permafrost and Periglacial Processes, 19: 195-210. DOI:10.1002/ppp.620

Montgomery, D.R. and Korup, O. (2011) Preservation of inner gorges through repeated Alpine glaciations. – Nature Geoscience, 4: 62–67.

Müller, B.U. (1999): Paraglacial sedimentation and denudation processes in an Alpine valley of Switzerland. An approach to the quantification of sediment budgets. – Geodinamica Acta, 12: 291-301.

Murton, J.B., Coutard, J.-P., Ozouf, J.-C., Lautridou, J.-P., Robinson, D.A. and Williams, R.B.G. (2001): Physical modelling of bedrock brecciation by ice segregation in permafrost. – Permafrost and Periglacial Processes, 12: 255–266.

Murton, J.B., Peterson, R. and Ozouf, J.-C. (2006): Bedrock fracture by ice segregation in cold regions. – Science, 314: 1127-1129.

Nemec, W. and Kazanci, N. (1999): Quaternary colluvium in west-central Anatolia: sedimentary facies and paleoclimatic significance. – Sedimentology, 46: 139-170.

Nicolussi, K., Kaufmann, M., Patzelt, G., van der Plicht, J. and Thurner, A. (2005): Holocene tree-line variability in the Kauner valley, central Eastern Alps, indicated by dendrochronological analysis of living trees and subfossil logs. – Vegetation History and Archaeobotany, 14: 221-234.

Nötzli, J. and Gruber, S. (2005): Alpiner Permafrost–ein Überblick. – Jahrbuch des Vereins zum Schutz der Bergwelt, 70: 111-121.

Norton, K.P., von Blanckenburg, F. and Kubik, P.W. (2010): Cosmogenic nuclide-derived rates of diffusive and episodic erosion in the glacially sculpted upper Rhone Valley, Swiss Alps. – Earth Surface Processes and Landforms, 35: 651-662.

Obanawa, H. and Matsukura, Y. (2006): Mathematical modeling of talus development. – Computers and Geosciences, 32: 1461–1478.

Ostermann, M. and Sanders, D. (2010): Proxy-dating the Tschirgant rock avalanche event with the U/Th method. – Geophysical Research Abstracts 12: EGU2010-24-1, 2010.

Pagliarini, L. (2008): Strukturelle Neubearbeitung des Tschirgant und Analyse der lithologisch-strukturell induzierten Massenbewegung (Tschirgant Bergsturz, Nördliche Kalkalpen, Tirol). – Unpubl. MSc thesis, Univ. of Innsbruck, 90 pp.

Patzelt, G. (1980): Neue Ergebnisse der Spät- und Postglazialforschung in Tirol. Jahresberichte der Österreichischen Geographischen Gesellschaft, 76/77: 11-18.

Patzelt, G. (1987): Untersuchungen zur nacheiszeitlichen Schwemmkegel- und Talentwicklung in Tirol. – Veröffentlichungen des Landesmuseums Ferdinandeum, 67: 93-123.

Patzelt, G. and Poscher, G. (1993): Bemerkenswerte geologische und quartärgeologische Punkte im Oberinntal und im äusseren Ötztal. – In: Arbeitstagung der Geologischen Bundesanstalt, Geologie des Oberinntaler Raumes, pp. 205-216.

Prager, C., Zangerl, C., Patzelt, G. and Brandner, R. (2008): Age distribution of fossil landslides in the Tyrol (Austria) and its surrounding areas. – Natural Hazards and Earth System Sciences, 8: 377-407.

Rapp, A. (1960): Recent development of mountain slopes in Kärkevagge and surroundings, Northern Scandinavia. – Geografiska Annaler, 42: 65-200.

Robinson, D.A. and Moses, C.A. (2011): Rock surface and weathering: Process and form. – In: Gregory, K.J. and Goudie, A.S. (eds.), The SAGE Handbook of Geomorphology. SAGE Publications, London, pp. 291-309.

Sadler, P.M. (1981): Sediment accumulation rates and the completeness of stratigraphic sections. – Journal of Geology, 89: 569-584.

Sadler, P.M. (1999): The influence of hiatuses on sediment accumulation rates. – GeoResearch Forum, 5: 15-40.

Sanders, D. (2010): Sedimentary facies and progradational style of a Pleistocene talus-slope succession, Northern Calcareous Alps, Austria. – Sedimentary Geology, 228: 271-283.

Sanders, D. (2012): Effects of deglacial sedimentation pulse, followed by incision: A case study from a catchment in the Northern Calcareous Alps (Austria). – E&G Quaternary Science Journal, 61: 16-31.

Sanders, D., Ostermann, M. and Kramers, J. (2009): Quaternary carbonate-rocky talus slope successions (Eastern Alps, Austria): sedimentary facies and facies architecture. – Facies, 55: 345-373.

Sanders, D. and Ostermann, M. (2011): Post-last glacial alluvial fan and talus slope associations (Northern Calcareous Alps, Austria): A proxy for Late Pleistocene to Holocene climate change. – Geomorphology, 131: 85-97.

Sass, O. (2010): Spatial and temporal patterns of talus activity–a lichenometric approach in the Stubaier Alps, Austria. – Geografiska Annaler, 92A: 375-391.

Sass, O. and Wollny, K. (2001): Investigations regarding Alpine talus slopes using ground-penetrating radar (GPR) in the Bavarian Alps, Germany. – Earth Surface Processes and Landforms, 26: 1071-1086.

Sass, O., Wetzel, K.-F. and Friedmann, A. (2006): Landscape dynamics of sub-alpine forest fire slopes in the Northern Alps. – Zeitschrift für Geomorphologie, Supplement, 142: 207-227.

Sass, O., Heel, M., Hoinkis, R. and Wetzel, K.-F. (2010): A six-year record of debris transport by avalanches on a wildfire slope (Ahrnspitze, Tyrol). – Zeitschrift für Geomorphologie, 54: 181-193.

Schmid, S.M., Fügenschuh, B., Kissling, E. and Schuster, R. (2004): Tectonic map and overall architecture of the Alpine orogen. – Eclogae geologicae Helvetiae, 97: 93-117.

Seong, Y.B., Owen, L.A., Caffee, M.W., Kamp, U., Bishop, M.P., Bush, A., Copland, L. and Shroder, J.F. (2009): Rates of basin-wide rockwall retreat in the K2 region of the Central Karakoram defined by terrestrial cosmogenic nuclide 10Be. – Geomorphology, 107: 254-262.

Summerfield, M.A. (1991): Global Geomorphology. Longman Scientific & Technical, Essex, 537 pp.

Tinner, W. and Theurillat, J.-P. (2003): Uppermost limit, extent, and fluctuations of the timberline and treeline ecoline in the Swiss Central Alps during the past 11,500 years. – Arctic, Antarctic, and Alpine Research, 35: 158-169.

Tinner, W. and Vescovi, E. (2005): Ecologia e oscillazioni del limite degli alberi nelle Alpi dal Pleniglaciale al presente. – Studi Trentini di Scienze Naturali, Acta Geologica, 82: 7-15.

Tushinskiy, (1966), cit. in Luckman (1977, p. 36) [Luckman, B.H. (1977): The geomorphic activity of snow avalanches. – Geografiska Annaler, 59A: 31-48.]

Utili, S. and Crosta, G.B. (2011): Modeling the evolution of natural cliffs subject to weathering: 2. Discrete element approach. – Journal of Geophysical Research, 116, F01017. doi:10.1029/2009JF001559

Van Husen, D. (1983): General sediment development in relation to the climatic changes during Würm in the eastern Alps. – In: Evenson, E.B., Schlüchter, C. and Rabassa, J. (eds.), Tills and Related Deposits. AA Balkema, Rotterdam, pp. 345-349.

Van Husen, D. (1987): Die Ostalpen in den Eiszeiten. – Geologische Bundesanstalt, Wien, 24 pp., 1 map.

Van Husen, D. (2004): Quaternary glaciations in Austria. – In: Ehlers, J. and Gibbard, P.L. (eds.), Quaternary Glaciations-Extent and Chronology. Developments in Quaternary Science 2. Elsevier, Amsterdam, pp. 1-13.

Walder, J. and Hallet, B. (1985): A theoretical model of the fracture of rock during freezing. – Geological Society of America Bulletin, 96: 336-346.

Walder, J.S. and Hallet, B. (1986): The physical basis of frost weathering: Toward a more fundamental and unified perspective. – Arctic and Alpine Research, 18: 27-32.

Wieczorek, G.F. and Jäger, S. (1996): Triggering mechanisms and depositional rates of postglacial slope-movement processes in the Yosemite Valley, California. – Geomorphology, 15: 17-31.

Wieczorek, G.F., Stock, G.M., Reichenbach, P., Snyder, J.B., Borchers, J.W. and Godt, J.W. (2008): Investigation and hazard assessment of the 2003 and 2007 Staircase Falls rock falls, Yosemite National Park, California, USA. – Natural Hazards and Earth System Science, 8: 421-432.

Willenbring, J.K. and von Blanckenburg, F. (2010): Long-term stability of global erosion rates and weathering during late-Cenozoic cooling. – Nature, 465: 211-214.

Manuscript submitted: 6.11.2012
Revised manuscript accepted: 6.12.201